

Analysis of *cis*-Difluoroethylene Ozonide by Microwave Spectroscopy and *ab Initio* Techniques: An Unusual Conformational Potential^{1a}

Kurt W. Hillig II,^{1b} Robert L. Kuczkowski,^{*1b} and Dieter Cremer^{1c}

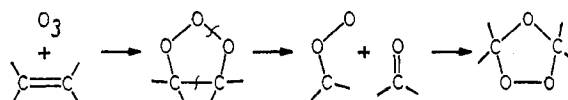
Department of Chemistry, University of Michigan, Ann Arbor, Michigan 48109, and Lehrstuhl für Theoretische Chemie, Universität Köln, D-5000 Köln 41, Federal Republic of Germany
(Received: September 22, 1983)

The microwave spectra of five isotopic species of *cis*-difluoroethylene ozonide (*cis*-3,5-difluoro-1,2,4-trioxolane) were assigned, including the parent, both the d_1 and the d_2 species, and the symmetric double-¹⁸O and the triple-¹⁸O species. A series of vibrational satellites also accompanied the ground-state transitions. The average structure consistent with this data was an ether oxygen envelope conformation having C_s symmetry, with the fluorines axial to the ring. *Ab initio* calculations were performed for selected values of the pseudorotational phase angle ϕ to provide additional insights. They indicated that the ether envelope corresponded to the minimum-energy conformer. The potential function vs. ϕ was relatively flat near the minimum and did not possess a low-energy path corresponding to the usual pseudorotation motion. Instead, the energy valley connecting puckered forms at 180, 90, and 270° terminates at the planar form. The ground-state conformation was discussed in terms of the balance between ring-substituent, substituent-substituent, and puckering forces. Stabilizing ring-substituent interactions dominate this interplay and are also reflected in long C-F and short C-O bond distances indicative of anomeric interactions involving the fluorine substituents.

Introduction

Since first being reported in 1868,² the reaction of ozone with alkenes in solution has been extensively studied by both experimental³ and theoretical⁴ means. While the mechanistic proposals have in general centered around that first put forth by Criegee⁵ (Scheme I), many of the refinements and alternative proposals have been based on presumed conformations of the intermediates and/or products.⁶ Reliable *ab initio* structural calculations of a few components of the reaction have recently been published.^{4a-c} Experimental structural information on the primary ozonide (1,2,3-trioxolane) and other intermediates is not available,⁷ and only five low molecular weight secondary ozonide (i.e. the 1,2,4-trioxolane product) structures have been reported. They include ethylene ozonide (EtOz),⁸ propylene ozonide (PrOz),^{6a} fluoroethylene ozonide (FOz),⁹ 1,1-difluoroethylene ozonide (3,3-difluoro-1,2,4-trioxolane, 1,1-F₂Oz),¹⁰ and cyclopentene

Scheme I



ozonide (6,7,8-trioxabicyclo[3.2.1]octane, CpOz).¹¹

The four monocyclic ozonides have nonplanar structures with large dihedral angles (40–50°) about the peroxy bond, while CpOz is constrained by its bicyclo[3.2.1]octane structure to a C_s symmetry conformation with a peroxy dihedral angle of 0°. Comparison of the structural data has revealed an interesting interplay between lone-pair, bond dipole, and anomeric interactions in determining the structure of the fluoro ozonides.^{9,10} The anomeric effect can be viewed as a delocalization of electron density from an oxygen atom lone-pair orbital into an adjacent C-X (X = O, F, N) σ^* orbital.¹² This orbital overlap is maximized when the C-X bond lies in a plane perpendicular to the C_X-O-R (R = O or C) plane, giving rise to the observed axial fluorine conformation in FOz and the O_H envelope conformation of 1,1-F₂Oz.¹³

The recent synthesis of *cis*-1,2-difluoroethylene ozonide (*cis*-3,5-difluoro-1,2,4-trioxolane, *c*-F₂Oz)¹⁴ provides an opportunity to further explore the interactions which affect ozonide structures. The anomeric effect should favor an O_{ether} (O_e) envelope form with the fluorines axial. However, the dipole-dipole repulsion across the ring of the C-F and C-O_{peroxy} (C-O_p) bonds as well as O_p lone-pair interactions will tend to distort the ring away from the symmetric ether envelope form. A previous theoretical study of this system found a broad energy minimum for pseudorotational phase angles (ϕ) from 90 to 180°, i.e. from roughly a peroxy-twisted half-chair form similar to EtOz to the O_e envelope with C_s symmetry. The calculated energy difference for the O_p envelope at $\phi = 108^\circ$ and the O_e envelope at $\phi = 180^\circ$ was only 70 cal/mol.

(10) K. W. Hillig II and R. L. Kuczkowski, *J. Phys. Chem.*, **86**, 1415-1420 (1982).

(11) D. G. Borseth and R. L. Kuczkowski, *J. Phys. Chem.*, **87**, 5381-5386 (1983).

(12) S. Wolfe, M.-H. Whangbo, and D. J. Mitchell, *Carbohydr. Res.*, **69**, 1-26 (1979); W. A. Szarek and D. Horton, Eds., "Anomeric Effect, Origin and Consequences", American Chemical Society, Washington, DC, 1979, ACS Symp. Ser. No. 87; R. U. Lemieux in "Molecular Rearrangements", P. deMayo, Ed., Interscience, New York, 1964.

(13) The nomenclature for substituent sites among the various ozonides is somewhat ambiguous; see ref 9, footnote 33. O_e refers to the ether oxygen, O_p will be used for the peroxy oxygen (O_H and O_F refer to peroxy oxygen atoms adjacent to CH₂ and CFX groups, respectively), etc. See also ref 15.

(14) C. W. Gillies, *J. Am. Chem. Soc.*, **99**, 7239-7245 (1977).

(15) D. Cremer, *J. Am. Chem. Soc.*, **103**, 3633-3638 (1981).

(1) (a) Portions of this work were presented as paper RB9, 37th Symposium on Molecular Spectroscopy, Ohio State University, Columbus, OH, 1982. (b) University of Michigan. (c) Universität Köln.

(2) C. F. Schönbein, *J. Prakt. Chem.*, **105**, 232 (1868).

(3) For reviews of the literature, see: R. W. Murray, *Acc. Chem. Res.*, **1**, 313 (1968); R. Criegee, *Angew. Chem.*, **87**, 765-771 (1975); P. S. Bailey, "Ozonation in Organic Chemistry", Academic Press, New York, 1978; R. L. Kuczkowski, *Acc. Chem. Res.*, **16**, 42 (1983).

(4) (a) D. Cremer, *J. Am. Chem. Soc.*, **103**, 3619-3626, 3627-3633 (1981); (b) *ibid.*, **101**, 7199-7205 (1979); (c) D. Cremer, *J. Chem. Phys.*, **70**, 1898-1910, 1911-1927, 1928-1938 (1979); (d) J. Renard and S. Fliszár, *J. Am. Chem. Soc.*, **92**, 2628 (1970); (e) R. A. Rouse, *ibid.*, **95**, 3460 (1973); (f) G. Klopman and P. Andreozzi, *Bull. Soc. Chim. Belg.*, **86**, 481 (1977); (g) G. Leroy and M. Sana, *Tetrahedron*, **32**, 1379 (1976); (h) P. C. Hilbert, *J. Am. Chem. Soc.*, **98**, 6088 (1976); (i) L. B. Harding and W. A. Goddard, *ibid.*, **100**, 7180-7188 (1978); (j) P. S. Nangia and S. W. Benson, *ibid.*, **102**, 3105-3115 (1980).

(5) R. Criegee, *Rec. Chem. Prog.*, **18**, 111-120 (1956).

(6) (a) R. P. Lattimer, R. L. Kuczkowski, and C. W. Gillies, *J. Am. Chem. Soc.*, **96**, 348-358 (1974); (b) P. S. Bailey and T. M. Ferrell, *ibid.*, **100**, 899-905 (1978); (c) G. D. Fong and R. L. Kuczkowski, *ibid.*, **102**, 4763-4768 (1980); U. Mazur, R. P. Lattimer, A. Lopata, and R. L. Kuczkowski, *J. Org. Chem.*, **44**, 3181-3185 (1979); U. Mazur and R. L. Kuczkowski, *ibid.*, **44**, 3185-3188 (1979).

(7) Structures of many aldehydes are of course known. 1,2-Dioxirane, an isomer of the carbonyl oxide "Criegee intermediate", has recently been identified and its structure determined: F. J. Lovas and R. D. Suenram, *Chem. Phys. Lett.*, **51**, 453-456 (1977); R. D. Suenram and F. J. Lovas, *J. Am. Chem. Soc.*, **100**, 5117-5122 (1978).

(8) (a) U. Mazur and R. L. Kuczkowski, *J. Mol. Spectrosc.*, **65**, 84-89 (1977); (b) R. L. Kuczkowski, C. W. Gillies, and K. L. Gallaher, *ibid.*, **60**, 361-372 (1976); (c) A. Almengen, P. Kolsaker, H. M. Seip, and T. Willadsen, *Acta Chem. Scand.*, **23**, 3398 (1969).

(9) K. W. Hillig II, R. P. Lattimer, and R. L. Kuczkowski, *J. Am. Chem. Soc.*, **104**, 988-993 (1982).

However, the calculations lacked a full geometry optimized treatment.

This paper reports microwave (MW) data for several isotopic species and an improved theoretical investigation which indicates that the O_e envelope conformer is at the energy minimum. The evidence also points to a low-frequency vibrational motion and a relatively flat pseudorotational potential function associated with the ground-state species.

Experimental Section

Instrumentation. All microwave spectra were recorded on a Hewlett-Packard 8460A spectrometer using radio frequency-microwave double resonance method (RFMWDR),¹⁶ with a Tektronix SG503 oscillator, a buffered Mini-Circuits Lab SGA-3 mixer, and an ENI 406L amplifier as the radio frequency modulation source. The spectrometer cell was cooled with dry ice to between -40 and -60 °C. While the spectrometer's intrinsic resolution is about 0.01 MHz, the large line width of $c\text{-F}_2\text{Oz}$ (typically about 1 MHz hwhm at a pressure of 20–30 mtorr) and its crowded spectrum allowed a measurement accuracy of only 0.1–0.3 MHz. The decomposition half-life of $c\text{-F}_2\text{Oz}$ of ≤ 20 min and the very low synthetic yields (vide infra) made it impractical to employ computerized signal-averaging techniques to enhance the spectral sensitivity and resolution.

Infrared spectra were recorded with a Beckman 4240 spectrometer; far-IR spectra were recorded with a hybrid Digilab interferometer. Syntheses and product workups were carried out on a preparative vacuum line using standard high-vacuum techniques. Chromatographic separations were performed on a Varian Aerograph 920 at room temperature with 30 mL/min of He as a carrier using an 8 ft \times $1/4$ in. 15% Dow Corning 710 on Chromosorb W column. A sampling loop to permit the direct injection of samples from the vacuum line was used.

Syntheses. *cis*-Difluoroethylene ozonide was typically made by reacting 3 mmol of *cis*-difluoroethylene (*c*-DFE; PCR Inc.) in 20–25 mmol of chlorotrifluoromethane (Matheson) at -95 °C, with 0.15–0.20 mmol/min of O_3 in O_2 from a Welsbach T-408 ozonator for 10–15 min by using standard techniques.⁹ All reactants were dried by passage through at -78 °C trap.

Deuterated *c*-DFE was prepared by exchange with 1 M NaOD/ D_2O in a stainless-steel bomb at 10 atm and 120 °C.⁹ Essentially complete exchange could be obtained in 2 days (as determined by gas-phase IR spectroscopy). $c\text{-F}_2\text{Oz-d}_2$ was prepared by ozonolysis of this material, while it was mixed 1:1 with *n*-DFE for the synthesis of $c\text{-F}_2\text{Oz-d}_1$. The latter reaction should yield a normal: d_1 : d_2 ozonide ratio of 1:0:1 in the limit of no scrambling (see Scheme I) and 1:2:1 for complete randomization. MW intensity measurements of the three species were roughly 1:2:1, indicative of considerable scrambling.

^{18}O -labeled species were made by using 98% $^{18}O_2$ (Mound Labs) in the ozone generator previously described.⁹ Triply substituted ^{18}O ozonide was prepared from $^{18}O_3$. The $^{18}O_p\text{-}^{18}O_p$ species was made by adding 5 mmol of HCOF (prepared by the method of Olah¹⁷) to the initial reaction mixture followed by about 1.3 mmol of $^{18}O_3$. In this synthesis, the MW spectra of the $^{18}O_3$ ozonide was several times weaker than those of the $^{18}O_p\text{-}^{18}O_p$ ozonide, indicative of considerable insertion of the added HCOF into the ozonide. This result (and the extensive deuterium scrambling mentioned above) indicates that the formation of the ozonide proceeds to a large extent via an "out-of-cage" Criegee mechanism.^{6c} Thus, the carbonyl oxide intermediate separates from the coproduced formyl fluoride and randomly recombines with the available aldehyde.

The reaction products were separated by trap-to-trap distillation through -78 and -196 °C traps. The major components of the -78 °C trap were *cis*-difluoroethylene oxide, *trans*-difluoroethylene ozonide, and $c\text{-F}_2\text{Oz}$. The *cis* ozonide was purified by vapor-phase

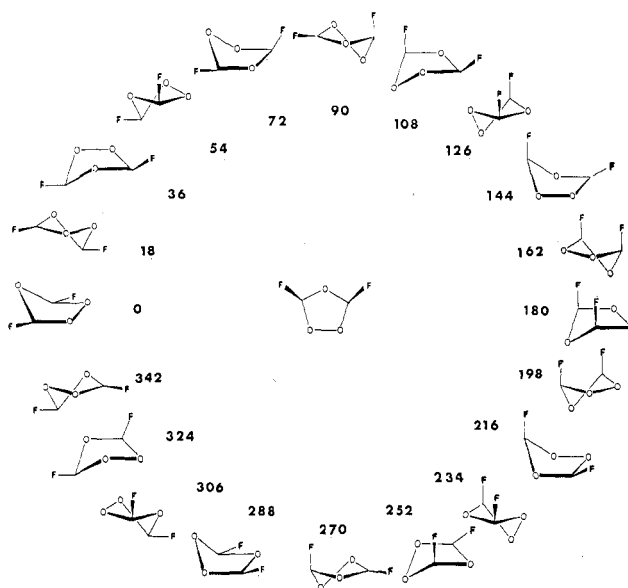


Figure 1. Pseudorotation itinerary of $c\text{-F}_2\text{Oz}$. Puckered conformers are shown at ϕ intervals of $\pi/10$ for $q > 0$.

chromatography. The overall yield of $c\text{-F}_2\text{Oz}$ relative to ozone was typically 1–2%. Samples were stored under vacuum in liquid nitrogen.

To minimize the risk of explosions,⁹ ozone input was limited to 2 mmol in any reaction. All reactions were carried out inside a Plexiglas shield fitted with remote control handles to the stopcocks.

Theoretical Methods. The conformational features of $c\text{-F}_2\text{Oz}$ are best described by its ring-puckering coordinates,¹⁸ namely the puckering amplitude q reflecting the degree of nonplanarity of the five-membered ozonide ring and the pseudorotation phase angle ϕ defining the mode of ring puckering. ϕ values of 0 and 180° correspond to the O_e envelope forms having the F atoms in equatorial (0°) or axial positions (180°) (see Figure 1). O_p envelope forms can be found at 72° (288°) and 108° (252°), and the O_pO_p twist forms at 90° (270°), where the ϕ values in parentheses belong to the enantiomeric conformers. The conformational energy function is symmetrical to the line $q > 0$, $\phi = 0$; $q = 0$; $q > 0$, $\phi = 180^\circ$, which is the location of all C_s -symmetrical $c\text{-F}_2\text{Oz}$ forms in q, ϕ space.

Equilibrium geometries, relative energies, and the conformational behavior of $c\text{-F}_2\text{Oz}$ have been calculated with the aid of standard restricted Hartree-Fock theory employing Pople's split valence 4-31G and augmented split valence 6-31G* basis sets.¹⁹ Previous calculations indicated that there is a strong dependency of the conformational energy on the F positions.¹⁵ The puckering amplitude, bond lengths, and angles couple strongly with changes of the F positions which in turn depend on ϕ .^{18b} Therefore, the semirigid pseudorotor model used in the first investigation of $c\text{-F}_2\text{Oz}$ was replaced by a flexible model²⁰ in which all parameters are relaxed for any change of ϕ .

Due to the computational demands of such an approach (calculations with 109 functions (6-31G* basis), optimization of 21 parameters!), we have simplified calculations using the following procedure: (1) For given values of ϕ we have optimized the amplitude q , bond lengths, and bond angles with the 4-31G basis utilizing previously obtained ozonide geometries^{4a,c} as suitable guess structures. The only parameters which are kept fixed at standard

(18) (a) D. Cremer and J. A. Pople, *J. Am. Chem. Soc.*, **97**, 1354–1357 (1975); (b) D. Cremer, *Isr. J. Chem.*, **20**, 12–19 (1980); (c) D. Cremer, RING, Quantum Chemical Program Exchange, Program No. 288, Bloomington, Indiana, 1977; D. Cremer and H. Essén, RING2, to be submitted for publication.

(19) (a) R. Ditchfield, W. J. Hehre, and J. A. Pople, *J. Chem. Phys.*, **54**, 724–728 (1971); (b) P. C. Hariharan and J. A. Pople, *Theor. Chim. Acta*, **28**, 213–222 (1973).

(20) D. Cremer, *Isr. J. Chem.*, in press.

(16) F. Wodarczyk and E. B. Wilson, Jr., *J. Mol. Spectrosc.*, **37**, 445–463 (1971).

(17) G. A. Olah and S. J. Kuhn, *J. Am. Chem. Soc.*, **82**, 2380–2382 (1960).

values are the CH bond lengths ($R_{\text{CH}} = 1.09 \text{ \AA}$). (2) At the second stage of the investigation the puckering amplitude and the internal ring angles have been reoptimized with the 6-31G* basis keeping all other parameters at 4-31G values. Theoretical values obtained in this way are known to provide a reasonable description of geometry and conformation of puckered rings.^{4a,c,20,21}

Results

Microwave Spectra. The Stark modulated spectrum of *c*-F₂Oz was very dense with no obvious patterns. Line widths were 1–2 MHz (fwhm) for sample pressures ≥ 15 mtorr, and many transitions appeared to be fully modulated with the Stark modulator output nominally at 0 V (actually ca. 20 V (base peak)). Due to the rich spectrum, Stark effects could not be clearly followed. This precluded the use of Stark splittings for spectral assignment and for measurement of the dipole moment.

The spectrum was greatly simplified by RFWDR and found to consist of several series of μ_v -dipole, Q-branch, K-doublet pairs, where the associated radio frequency transition is μ_c -dipole allowed. One intense vibrational satellite series with a similar pattern was interwoven with the ground-state pattern. A second weaker vibrational satellite was eventually identified as well as a few of the more intense transitions in approximately the expected positions for a third higher satellite. However, the ozonide samples were depleted before the second and third series could be fully examined at high resolution. While more than 16 of the ground-state, Q-branch pairs could be seen, only three R-branch, K-doublet pairs occur between 26.5 and 40 GHz in the DR spectrum. No other R-branch lines could be unambiguously identified by Stark modulation. The assigned transitions of the ground vibrational state of *c*-F₂Oz are listed in Table I. The rotational and centrifugal distortion constants derived for the ground state are listed in Table II.

The centrifugal distortion analyses (P^4 terms) were performed using a modified version of Kirchhoff's program CDIST.²² The effects of centrifugal distortion led to shifts of up to 140 MHz at $J = 31$. These are not unusually large effects, so it was puzzling that occasional transitions could not be fit to better than 0.5–1.5 MHz by using the quartic centrifugal distortion treatment. (This held true also for the vibrational satellites and the enriched isotopic species.) In some cases this was obviously due to overlapping by weaker neighboring lines, but other deviate transitions appeared free of interference and had symmetric line shapes of ~ 1 MHz (hwhm). A misassignment of the Q-branch series by one or two units in J was explored but seemed improbable.

The possibility of a vibration-rotation perturbation arising from a small barrier-double minimum type of potential function was considered but rejected on the basis of the ab initio calculations described below. These calculations and the presence of a low-lying vibrational state in the MW spectra indicate that a rather low-frequency, presumably large-amplitude motion is associated with the ring pseudorotation coordinate. It appears that this motion is the likely origin for the small residual deviations in the spectral fit. The limited data set did not make it worthwhile to incorporate P^6 distortion terms or other modeling schemes in order to further improve the fit.

The rotational and centrifugal distortion constants derived from the most intense vibrational satellite are listed in Table II as the $v = 1$ state. For the $v = 2$ state, no R-branch transitions could be assigned and only $A-C$ and κ were determined; the regular change in their values suggests the assignment to the second excitation of the same mode as the $v = 1$ state. (The transition frequencies are available as supplementary tables.) Since the dipole moment was not determined, an estimate of the energy difference between the $v = 0$ and 1 levels was made by measuring the change in relative intensity ratios of several pairs of transitions

TABLE I: Assigned Transitions of the Normal Isotopic Species of *cis*-Difluoroethylene Ozonide (*c*-F₂Oz) in the Ground State

transition	$\nu_{\text{obsd}}/\text{MHz}$	centrifugal distortn cor	obsd - calcd
6(0,6) ← 5(1,5)	29 155.48	-0.166	-0.113
6(1,6) ← 5(0,5)	29 291.70	-0.243	0.292
7(0,7) ← 6(1,6)	33 890.20	-0.237	0.034
7(1,7) ← 6(0,6)	33 942.32	-0.285	0.125
8(0,8) ← 7(1,7)	38 599.68	-0.313	-0.383
8(1,8) ← 7(0,7)	38 619.13	-0.341	-0.010
19(4,15) ← 19(3,16)	29 964.60	-28.658	0.386
19(5,15) ← 19(4,16)	30 013.60	-29.032	-0.596
19(6,14) ← 19(5,15)	26 884.50	-33.161	1.307
20(4,16) ← 20(3,17)	32 155.40	-32.486	0.219
20(5,16) ← 20(4,17)	32 176.50	-32.687	0.229
20(5,15) ← 20(4,16)	28 783.06	-35.749	0.111
20(6,15) ← 20(5,16)	29 038.89	-37.323	-0.091
21(5,16) ← 21(4,17)	31 105.50	-40.931	0.323
21(6,16) ← 21(5,17)	31 222.20	-41.862	-0.315
22(6,16) ← 22(5,17)	29 620.32	-48.138	-0.042
22(7,16) ← 22(6,17)	30 140.05	-51.489	-0.024
23(6,17) ← 23(5,18)	32 083.95	-55.147	0.108
23(7,17) ← 23(6,18)	32 334.27	-57.229	-0.140
24(5,19) ← 24(4,20)	37 765.45	-57.363	0.834
24(6,19) ← 24(5,20)	37 774.60	-57.506	0.633
24(6,18) ← 24(5,19)	34 433.49	-62.227	0.128
24(7,18) ← 24(6,19)	34 549.27	-63.445	-0.152
25(6,19) ← 25(5,20)	36 713.53	-69.423	-0.029
25(7,19) ← 25(6,20)	36 765.45	-70.101	-0.136
25(7,18) ← 25(6,19)	32 866.63	-71.084	-0.182
25(8,18) ← 25(7,19)	33 362.17	-75.351	0.133
26(6,20) ← 26(5,21)	38 951.20	-76.794	0.197
26(7,20) ← 26(6,21)	38 973.06	-77.156	-0.630
26(7,19) ← 26(6,20)	35 353.91	-80.323	0.125
26(8,19) ← 26(7,20)	35 593.85	-82.935	0.046
27(7,20) ← 27(6,21)	37 729.00	-89.582	1.822
27(8,20) ← 27(7,21)	37 840.00	-91.098	0.713
28(7,21) ← 28(6,22)	40 031.00	-98.943	0.654
28(8,21) ← 28(7,22)	40 081.00	-99.783	-0.131
28(8,20) ← 28(7,21)	36 090.43	-100.240	-0.074
28(9,20) ← 28(8,21)	36 555.34	-105.444	0.071
29(8,21) ← 29(7,22)	38 596.83	-112.000	0.248
29(9,21) ← 29(8,22)	38 822.79	-115.147	0.040
31(9,22) ← 31(8,23)	39 293.09	-136.335	-0.084
31(10,22) ← 31(9,23)	39 724.06	-142.463	-0.025

between 25 and -40 °C. The results indicate that the first excited vibrational state lies $60 \pm 50 \text{ cm}^{-1}$ above the ground state. An effort was made to observe transitions associated with this mode using a far-IR spectrometer; however, the ozonide completely decomposed during the spectral acquisition period of 90 min. Strong HCOF bands were observed in the spectrum, and several weak features also occurred between 30 and 100 cm^{-1} , but it was difficult to unambiguously assign them to the ozonide.

Spectra were assigned for the $v = 0$ and 1 states of the di-deuterio species and the $v = 0$ states of the monodeuterio, triple-¹⁸O, and double-¹⁸O_p¹⁸O_p species by using the RFWDR technique. Only one ground-state spectrum was found for the d_1 ozonide species. This suggests that the ground state has C_s symmetry since an asymmetric structure would give two distinguishable isomers, i.e. d_{axial} and $d_{\text{equatorial}}$. The transitions of the d_1 species were roughly twice as intense as those of either the d_0 or d_2 species in that sample (vide syntheses), which is also supportive of C_s symmetry. The rotational and distortion constants obtained for all of the assigned species are listed in Table II. A complete list of the assigned transitions of all of the species is available (Tables S1–S7, supplementary material).

Conformation and Structure. Spectral Analyses. One test for the presence or absence of symmetry has already been seen in the qualitative appearance of the d_1 ozonide spectrum. A further test of symmetry lies in the comparison of the hydrogen atom coordinates by Kraitchman's method²⁴ for single substitution (which is independent of symmetry) and by the Chutjian-Nygaard

(21) (a) D. Cremer and J. A. Pople, *J. Am. Chem. Soc.*, **97**, 1358–1367 (1975); (b) D. Cremer, *ibid.*, **99**, 1307–1309 (1977); (c) D. Cremer, O. V. Dorofeeva, and V. S. Mastryukov, *J. Mol. Struct.*, **75**, 225–240 (1981).

(22) W. H. Kirchhoff, *J. Mol. Spectrosc.*, **41**, 333–380 (1972). τ_3 is defined according to eq 13 rather than the alternative proposed by Watson.²³

(23) J. K. G. Watson, *J. Chem. Phys.*, **46**, 1935–1949 (1967).

(24) J. Kraitchman, *Am. J. Phys.*, **21**, 17–24 (1953).

TABLE II: Rotational and Centrifugal Distortion Constants of $c\text{-F}_2\text{Oz}$

	$n\text{-F}_2\text{Oz}$			$\text{F}_2\text{Oz-d}_2$		$^{18}\text{O}_p\text{-}^{18}\text{O}_p\text{-F}_2\text{Oz}$	$^{18}\text{O}_3\text{-F}_2\text{Oz}$	
	$\nu=0$	$\nu=1$	$\nu=2$	$\text{F}_2\text{Oz-d}_1$	$\nu=0$			$\nu=1$
A''/MHz	4256.68 (11) ^a	4292.70 (15)		4219.33 (23)	4179.85 (16)	4212.97 (28)	4052.69 (47)	3963.35 (77)
B''/MHz	2923.67 (4)	2898.32 (4)		2843.41 (4)	2776.82 (5)	2744.11 (3)	2882.34 (7)	2842.79 (7)
C''/MHz	2347.38 (4)	2339.67 (3)		2304.95 (3)	2264.06 (5)	2257.21 (3)	2266.26 (3)	2263.23 (4)
τ_1/kHz	-29.9 (4.6)	-23.2 (5.6)		-37.2 (4.3)	-35.0 (5.0)	-32.0 (4.4)	-45.1 (6.6)	-36.8 (8.1)
τ_2/kHz	-7.4 (1.5)	-6.2 (1.7)		-9.9 (1.4)	-9.4 (1.6)	-8.8 (1.3)	-11.8 (1.9)	-9.9 (2.4)
τ_3/kHz	0.00	0.00		0.01	0.00	0.00	0.08	0.26
τ_{aaaa}/kHz	-10.8 (6.5)	-18.0 (15)		-5.3 (7.7)	-7.0 (5.5)	9.3 (9.6)	11.9 (12)	-12.0 (13)
τ_{bbbb}/kHz	-4.7 (1.3)	-7.7 (1.1)		-6.6 (1.2)	-6.7 (1.6)	-7.4 (1.0)	-6.1 (1.1)	-6.9 (1.2)
τ_{cccc}/kHz	-0.25 (1.3)	-2.4 (1.1)		-2.5 (1.2)	-3.0 (1.6)	-2.6 (1.0)	-1.3 (1.1)	-3.4 (1.3)
$A-C$	1909.30	1953.03	1990.72		1915.79	1955.76		
κ	-0.396	-0.428	-0.449		-0.475	-0.502		
no. of lines	41	42	25	26	39	29	23	22

^a The number in parentheses represents one standard deviation in the fit.

TABLE III: Substitution Coordinates of the Hydrogen Atom

coord	Kraitchman ^a	Chutjian-Nygaard ^b	K-CN
a	± 1.9651	± 1.9649	0.0002
b	0.2662	0.2715	-0.0053
c	1.0137	1.0149	-0.0012

^a Calculated from the d_0 and d_1 species.²⁰ ^b Calculated from the d_0 and d_2 species.²¹

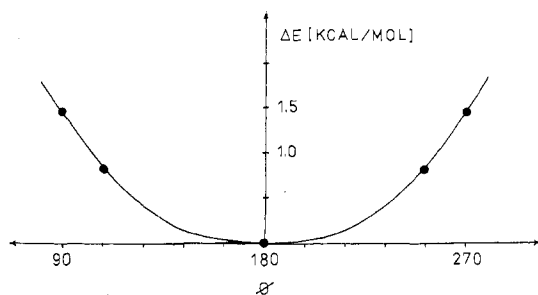


Figure 2. Theoretical pseudorotational potential between $\phi = 90$ and 270° . The solid line gives the energy change along the dashed line of Figure 4.

method²⁵ for symmetric double substitution (using the d_2 species). If the molecule has a plane of symmetry, then the two sets of coordinates should be essentially identical. The results, shown in Table III, coincide within 0.0012 Å for the a and c coordinates and differ by only 0.0053 Å for the smaller and more uncertain²⁶ b coordinate. The excellent agreement confirms the C_s symmetry of the ground state of $c\text{-F}_2\text{Oz}$.

Insufficient isotopic data are available to completely determine the structure by the Kraitchman and Chutjian methods, since carbon and fluorine substitution data are not available. (An enriched ^{13}C synthesis was not practical given the low yields.) In principle, the structure can be calculated by a least-squares fit of the 14 Cartesian coordinates (assuming C_s symmetry) to the 14 equations derived from the observed moments of inertia, the center of mass, and the product of inertia equations. This yields the " r_0 " or effective structure. In practice such a minimum data set often leads to implausible structures due to the cumulative errors introduced by neglecting small differences in the vibrational amplitudes of the isotopic species, differences in the set of transitions used in calculating rotational constants, etc. It was therefore not surprising, given the evidence for low-frequency, large-amplitude motion, that such r_0 calculations would not successfully converge in this case.

An alternative procedure called the method of "predicate observables"^{27,28} was employed to estimate structural parameters

TABLE IV: Comparison of Structural Parameters Obtained for $c\text{-F}_2\text{Oz}$ and EtOz ^a

parameter	$c\text{-F}_2\text{Oz}$			EtOz	
	MW ^b	ab initio ^c		MW ^d	ab initio ^e
		flexible	semirigid		
ϕ	180	180	180	90	90
q	0.263	0.282	0.362	0.464	0.456
$\alpha_{\text{F}_{\text{ax}}}$ ^f	17.3	17.1	11.1	14.6	16.9
$\alpha_{\text{H}_{\text{eq}}}$	123.2	125.1	120.7	126.3	125.9
C-O _e	1.385	1.396	1.415	1.416	1.426
C-O _p	1.376	1.407	1.439	1.412	1.433
O _p -O _p	1.468	1.476	1.476	1.461	1.467
C-F	1.376	1.366	(1.36)	1.10	(1.09)
C-H	1.091	(1.09)	(1.09)	1.09	(1.09)
F...F	1.912	2.942	2.782		
$\angle \text{CO}_e\text{C}$	105.3	106.8	103.8	104.8	106.5
$\angle \text{O}_e\text{CO}_p$	107.4	105.7	104.9	105.5	104.6
$\angle \text{CO}_p\text{O}_p$	105.5	105.8	105.1	99.3	100.1
$\angle \text{O}_e\text{CF}$	109.3	110.3	109.6	109.8	110.8
$\angle \text{O}_e\text{CH}$	111.8	111.5	111.9	110.8	110.5
$\angle \text{O}_p\text{CF}$	109.7	110.0	109.3	109.8	111.7
$\angle \text{O}_p\text{CH}$	112.4	111.0	110.5	106.7	108.7
$\angle \text{HCF}$	106.2	108.3	110.5	113.3	110.4
$\angle \text{CO}_p\text{O}_p\text{C}$	0	0	0	49.5	48.5
$\angle \text{O}_p\text{O}_p\text{CO}_e$	18.1	18.7	23.6	40.8	39.6
$\angle \text{O}_p\text{CO}_e\text{C}$	29.5	31.2	38.8	16.2	15.6
$\angle \text{O}_p\text{O}_p\text{CF}_{\text{ax}}$	100.7	100.4	93.8	77.7	80.3
$\angle \text{CO}_e\text{CF}_{\text{ax}}$	89.5	87.7	78.4	102.7	104.9
$\angle \text{O}_p\text{O}_p\text{CH}_{\text{eq}}$	141.5	139.8	144.4	158.7	159.4
$\angle \text{CO}_e\text{CH}_{\text{eq}}$	153.3	151.9	158.7	131.3	136.1

^a Distances in angstroms, angles in degrees; parameters in parentheses are not optimized. ^b Calculated by least-squares fitting of spectral data and predicate observables (see text and ref 28 and 29). ^c Total energies are -500.251 09 (flexible pseudorotor) and -500.243 16 hartree (semirigid pseudorotor). ^d Reference 8b; only parameters for the axial F and the equatorial H are given. ^e Reference 4a; see comment c. ^f For the definition of the substituent orientation angle, see ref 15b.

consistent with the spectral data. In this procedure, additional constraints (i.e. assumptions about structural parameters) are added to the least-squares fitting as "pseudoexperimental" data with attached uncertainties or weights rather than as fixed values. A number of calculations were explored for a variety of input assumptions and weighting factors. One of these resultant fits

(27) L. S. Bartell, D. Romanesko, and T. C. Wong, *Spec. Period. Rep.: Mol. Struct. Diff. Methods*, 3, Chapter 4 (1975). See also: P. Nösberger, A. Bauder, and Hs. H. Günthard, *Chem. Phys.*, 1, 418-425 (1973); J. J. Kierns and R. F. Curl, Jr., *J. Chem. Phys.*, 48, 3773-3779 (1968).

(28) All structural calculations were performed with our extended version of Schwendeman's STRFIT program; R. Schwendeman in "Critical Evaluation of Chemical and Physical Structural Information", D. R. Lide and M. A. Paul, Eds., National Academy of Sciences, Washington DC, 1974, pp 74-115. The conversion factor used between rotational constants and moments of inertia was 505 379.05 amu Å² MHz.

(25) L. Nygaard, *J. Mol. Spectrosc.*, 62, 292-293; A. Chutjian, *ibid.*, 14, 361-370 (1964).

(26) C. C. Costain, *J. Chem. Phys.*, 29, 864-874 (1958).

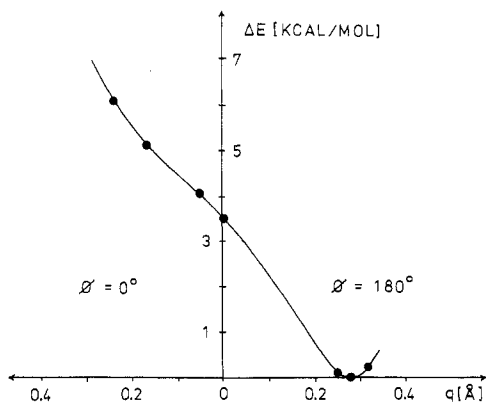


Figure 3. Theoretical inversion potential of the equilibrium form ($\phi = 180^\circ$; axial F atoms) of $c\text{-F}_2\text{Oz}$. $\phi = 0^\circ$ corresponds to the O_e envelope with equatorially positioned F atoms.

termed the MW structure is listed in Table IV.²⁹ However, other acceptable fits ($I_{\text{obsd}} - I_{\text{calcd}} \leq 0.06 \text{ amu } \text{\AA}^2$) could also be obtained where the bond lengths varied as much as $\pm 0.02 \text{ \AA}$. Consequently, the ground-state moments of inertia are consistent with plausible parameters (see Discussion) but are not sufficient for estimating very precise structural details. Corrections to the moments of inertia due to the low-frequency vibrational motion are probably necessary in order to improve the structural analysis.

Ab Initio Analysis. Ab initio calculations with the flexible pseudorotor model clearly demonstrate the existence of an energy minimum at $\phi = 180^\circ$, i.e. for an O_e envelope conformation with axially positioned F atoms (Figure 1). The conformational potential is rather flat between $\phi = 90$ and 270° as indicated in Figure 2. The calculated energy difference of about 1.5 kcal/mol between the O_e envelope form at 180° and the two O_pO_p twist forms at 90 and 270° implies the presence of a low-frequency, large-amplitude vibrational mode in the ground state.

No other minimum than the one at $\phi = 180^\circ$ can be found when varying ϕ from 0 to 360° . Contrary to other alkene ozonides investigated so far,^{4a,c} the planar form of $c\text{-F}_2\text{Oz}$ is no longer a local energy maximum in q, ϕ space. When the puckering amplitude of the O_e envelope form at $\phi = 180^\circ$ is reduced, the relative energy increases to 3.5 kcal/mol at $q = 0$ (planar $c\text{-F}_2\text{Oz}$) and continues to increase if the molecule inverts to an O_e envelope with equatorially positioned F atoms ($\phi = 0^\circ$; Figure 3). The inverted envelope with $q = 0.28 \text{ \AA}$ is about 8 kcal/mol less stable than the equilibrium conformation at 180° ; i.e., ring inversion is no longer a preferred conformational mode of the ozonide ring. Also, there exists no minimum-energy path for pseudorotation of $c\text{-F}_2\text{Oz}$. The energy valley connecting puckered forms at $\phi = 180, 90,$ and 270° terminates at the location of the planar form as indicated in Figure 4.

The structural parameters corresponding to the minimum energy conformation are listed in Table IV, both for the flexible and semirigid pseudorotor model. Comparison of these data with the MW structure underlines the necessity of a full geometry optimization (flexible pseudorotor) and reveals structural changes caused by the F substituents. These changes become even more apparent when considering results obtained for EtOz, which are also included in Table IV.

The puckering amplitude of $c\text{-F}_2\text{Oz}$ is reduced by almost 40% as compared to that of EtOz. This is due to both the change of ϕ from 90° (EtOz) to 180° and dipole-dipole repulsion between the CF bond moments across the ring. The decrease of the

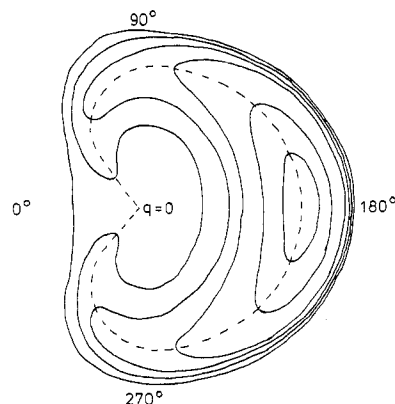


Figure 4. Qualitative conformational surface of $c\text{-F}_2\text{Oz}$ given by a contour line diagram. The center with $q = 0$ is the location of the planar form. The dashed line corresponds to the energetically most favorable conformational change of the equilibrium form.

puckering amplitude from 0.36 \AA (semirigid pseudorotor) to 0.28 \AA leads to an increase of the F-F distance from 2.78 to 2.94 \AA and hence a lowering of dipole-dipole repulsion.

The change in ϕ leads to a small lengthening of the O_pO_p bond, which is due to enhanced lone pair-lone pair (1p-1p) repulsion in the O_e envelope form. There is no further change of this parameter when the semirigid pseudorotor model is relaxed; i.e., the O_pO_p bond length couples only weakly with q or the CF bond lengths. However, strong coupling is found between CO and CF bond lengths. The former decrease by $0.02\text{--}0.03 \text{ \AA}$, which is indicative of significant anomeric interactions involving C, O, and F atoms.

Comparison of ab initio and experimental results obtained for $c\text{-F}_2\text{Oz}$ reveals that agreement is similar to the case of EtOz, where extensive spectral data and ab initio calculations are available.^{4c,8a,8b} The parameters obtained from spectral constants are essentially effective (r_0) parameters and contain effects of averaging over the ground vibrational state. Thus, a comparison with the r_e values of the ab initio calculations can only be done qualitatively. On this basis, three observations can be made: (1) Both experiment and theory agree with regard to the overall shape of $c\text{-F}_2\text{Oz}$. This is reflected by the ϕ , the q , and the substituent position angles^{18b} listed in Table IV. Puckering is calculated to be somewhat larger than expected from spectroscopic data. (2) Calculated ring bond lengths are $0.01\text{--}0.03 \text{ \AA}$ longer than the experimental ones, which is consistent with results found for EtOz (Table IV). (3) Theory predicts the CO_e length to be shorter than the CO_p length, which is contrary to estimates from the spectroscopic measurements. Due to the lack of suitable reference data, this contradiction cannot be resolved at present.

Discussion

Both experiment and theory indicate that $c\text{-F}_2\text{Oz}$ adopts an O_e envelope form in the ground state with both F atoms in axial positions. This conformation is the result of an interesting interplay of various electronic effects:

(1) The ozonide ring puckers in order to reduce lp-lp electron repulsion in the peroxide bridge. This would be best accomplished with a twist puckering mode which allocates a large dihedral angle about the O_pO_p bond. The same prediction can be made by examining the delocalized MOs of the ring. The antibonding character of the ozonide HOMO is strongly reduced for the O_pO_p twist but not for the O_e envelope forms.^{4c}

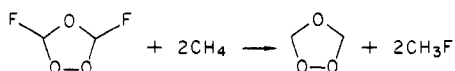
(2) Interaction of the F substituents with the ring forces the molecule to deform to the O_e envelope conformation. F is both a σ -acceptor and a π -donor substituent. Its donor capacity would lead to a population of the antibonding ozonide orbitals and hence to an overall destabilization of the molecule, provided its $2p\pi$ orbitals could overlap with the ring position. This is possible in an equatorial but not in an axial position.^{4c,15} Accordingly, a diaxial arrangement of the F substituents leads to the most stable while a diequatorial arrangement to the least stable $c\text{-F}_2\text{Oz}$

(29) The predicate observables used in this calculation were $d(\text{C-O}_e) = d(\text{C-O}_p) = 1.38 \text{ \AA}$, $d(\text{O-O}) = 1.470 \text{ \AA}$, $d(\text{C-F}) = 1.375 \text{ \AA}$, and $d(\text{C-H}) = 1.090 \text{ \AA}$. $(I_{\text{obsd}} - I_{\text{calcd}})_{\text{rms}}$ was $0.021 \text{ amu } \text{\AA}^2$, and the maximum deviation for any isotopic species was $0.039 \text{ amu } \text{\AA}^2$. In this calculation $d(\text{O-O})$ was weighted 20 times greater than the other bond lengths to constrain it close to a value typical of other ozonides. If $d(\text{O-O})$ was not weighted heavily, values as low as 1.45 \AA would result. Presumably, the low-frequency vibrational motion which deforms the ring from C_2 symmetry leads to the apparent short value of $d(\text{O-O})$.

conformers (Figure 3). As pointed out in the Introduction, this situation can be described in terms of localized orbitals via the anomeric effect: Both the O_e and O_p lp orbitals are almost coplanar (see dihedral angles in Table IV) with the CF bond and can therefore interact with the σ^*_{CF} orbital. This causes a shortening of the CO bonds and a lengthening of the CF bond. The latter effect becomes obvious when comparing the CF bond lengths found for *c*-F₂Oz (Table IV) with those of CHF₃ ($R_{CF} = 1.332 \text{ \AA}^{30}$), where the O atoms of the -O-CFH-O- fragment are replaced by additional F atoms. The difference (0.04 Å) clearly reveals a lengthening of the CF bond in *c*-F₂Oz.

(3) Once the molecule is "locked" in the diaxial O_e envelope form by strong ring-substituent interactions, puckering should increase in order to delocalize O_p lp electrons into the σ^*CO_e orbitals and thus to reduce lp-lp repulsion in the O_pO_p bridge. Puckering, however, leads to an increase of across ring interactions between the F atoms. Both monopole-monopole as well as dipole-dipole interactions are repulsive. Lowering of these interactions can be achieved either by a rocking motion of the CFH groups, a flattening of the puckered ring, or a combination of both effects. The calculated as well as the spectroscopic rocking angles are small (1.0 vs. 2.5°) as are the wagging (0.1 vs. 0.0°) and bending angles (0.4 vs. 0.5°). Hence, a reduction in the destabilizing electrostatic interactions between the F atoms is solely achieved by decreased puckering, although this will lead to enhanced antibonding in the HOMO of the ozonide.

The balance between ring-substituent, substituent-substituent, and puckering forces determines the actual values of the geometrical parameters. Stabilizing ring-substituent interactions clearly dominate which becomes obvious when considering the formal reaction³¹



The calculated reaction energy of 35.1 kcal/mol is the sum of four terms: twice a contribution of 22 kcal/mol which is due to stabilizing interactions between one F atom and the ring as obtained from the HF/6-31G* energy of monofluorozone;¹⁵ a gain of about 4 kcal/mol caused by changing the puckering mode of the ozonide from $\phi = 180$ to 0° (3 kcal/mol^{4c}) and increasing q from 0.28 to 0.35 Å (1 kcal/mol^{4c}); a destabilization term due to F-F interactions, which can be evaluated from the following equation:

$$35 = 2(22) - 4 + X \quad X = -5 \text{ kcal/mol}$$

A similar value is obtained when relaxing the semirigid pseudorotor model. Therefore, it is reasonable to say that F-F interactions destabilize *c*-F₂Oz by 5 kcal/mol.

It is interesting to note that energetic and geometrical results do not provide any indication that F-F interactions might be stabilizing. Through-space interactions between F atoms have been considered to be stabilizing in the case of 1,2-difluoroethylene (F₂Et) in order to rationalize the higher stability of its *cis* isomer as opposed to that of its *trans* isomer.³² In the equilibrium conformation *c*-F₂Oz contains the CF bonds in almost the same geometrical arrangement as in *c*-F₂Et (F-F distance 2.84 Å³²) separated, however, by two bonds rather than one. The absence of stabilizing F-F interactions in *c*-F₂Oz strongly suggests that

these depend on the type and number of bonds connecting the F atoms (F-C=C-F in F₂Et as opposed to F-C-O-C-F in F₂Oz); i.e., F-F attraction is a through-bond rather than a through-space phenomenon.³³ Work is in progress to further scrutinize this conclusion.

The features of the calculated conformational energy surface reflect the dominance of substituent-ring interactions in the ring. A gradual change of ϕ from 180 to 90 or 270° brings one F atom into an equatorial position (Figure 1 and ref 4c) and, hence, raises the energy. A situation where both F atoms are in an equatorial position ($\phi = 0^\circ$) is energetically less favorable (due to π -donation) than a planar form with the F substituent in an inclinal position, which does not allow the F atoms to develop their full donor capacity. For each conformer in q, ϕ space, opposing electronic effects determine geometry and stability as discussed for the equilibrium conformation. This leads to a conformational energy surface with potentially interesting dynamical effects. This was evident from the microwave spectrum which in fact motivated us to reexamine the energy surface by ab initio means for guidance on the presence of another low-energy form or for the presence of a small barrier at the C_s ($\phi = 180^\circ$) position. It would be interesting to obtain additional IR and MW data to further explore the vibration-rotation interaction effects associated with the pseudorotation coordinate. Unfortunately, the very inefficient syntheses of *c*-F₂Oz and its instability make it a very difficult experimental system to acquire the extensive spectral data necessary for this task.

c-F₂Oz is the second example of an ozonide possessing a stable O_e envelope conformation. The only previous example, however, occurs in cyclopentene ozonide where the bicyclic ring system constrains the ozonide ring to the C_2 -symmetrical envelope form.¹¹ The preference of a F substituent to adopt an axial position in the ozonide ring has already been demonstrated in vinyl fluoride ozonide⁹ and vinylidene fluoride ozonide.¹⁰ The geometrical data obtained in this work, in particular the spectrally derived CO and CF bond lengths, are very close to the r_0 values derived from the MW data on vinyl fluoride ozonide.¹⁹ In essence, the spectral and ab initio geometry parameters of *c*-F₂Oz most likely fit reasonable and systematic trends compared to the case for analogous systems.

In summary, *c*-F₂Oz is an unusual species providing nonroutine challenges to a spectroscopic or ab initio analysis. By combining both approaches, its ground-state conformation was established and structural parameters were estimated. This provided insight on the interplay between various electronic interactions which give rise to the uncommon conformational potential function. One noteworthy finding has been the indication that the F-F through-space interactions are basically repulsive unlike other examples such as *cis*-CHF=CHF where attractive or stabilizing F-F interactions occur which are apparently dependent on a through-bond mechanism.

Acknowledgment. This work was supported by Grants CHE-8005471 and CHE-8303615 from the National Science Foundation. Support at the Universität Köln was provided by the Deutsche Forschungsgemeinschaft and the Fond der Chemischen Industrie. All ab initio calculations were carried out at the Rechenzentrum der Universität Köln.

Supplementary Material Available: Tables S1-S7 listing transition frequencies for the ground and excited vibrational states (7 pages). Ordering information is given on any current masthead page.

(30) A. Yokozeki and S. H. Bauer, *Top. Curr. Chem.*, **53**, 71-119 (1975).

(31) The following absolute HF/6-31G* energies (in hartree) have been used to calculate the reaction energy: -500.25109 (*c*-F₂Oz), -40.19517 (CH₄), -302.51623 (EtOz), -139.03461 (CH₃F).

(32) D. Cremer, *Chem. Phys. Lett.*, **81**, 481-485 (1981), and references cited therein.

(33) R. C. Bingham, *J. Am. Chem. Soc.*, **98**, 535-540 (1976).